Influence of micro-crack on the propagation of a semi-infinite crack

Hamid Hamli Benzahar[1], Abderrazak SAID[2], and Mohamed CHABAAT[3]

[1]University of Djillali Bounaama
[2]Affiliation not available
[3]USTHB

August 4, 2020

Abstract

The main objective of this research is to determine the influence of micro-crack on the propagation of a semi-infinite crack. This study is mainly based on the determination of the strain energy during the interaction between the semi-infinite crack and the neighboring microcrack. The problem is formulated by a plane element, having a micro-crack varies around itself and around a semi-infinite crack. The cracked element is subjected to a uniform load according to mode I. The theoretical analysis of the strain energy is based on the stress found during the propagation of the semi-infinite crack. During the positioning of the micro-crack with respect to the semi-infinite crack, according to the strain energy results, the presence of the micro-crack can amplify, reduce and sometimes arrest the propagation of the semi-infinite crack.

I. Introduction

The interaction between the semi-infinite crack and a neighboring micro-crack has been studied by several researchers [1-3]. In this paper, based on the strain energy, this study is devoted to determining the influence of microcrack on the semi-infinite crack. During the propagation of semi-infinite crack, the strain energy is mainly based on the stress field found by H. Hamli benzahar [4]. The problem is formulated by a brittle material of a thin thickness, cracked at the end, having a microcrack varies around itself by an angle α and around d the semi-infinite crack by an angle (see Figure 1). The cracked model is subjected to a uniform load making opening of semi-infinite crack according to the first mode of rupture (Mode I). Using the mathematical approaches, the constraints and strains fields of a micro-crack and semi-infinite crack are formulated by using of the complex potentials theory [5]. The strain energy rate is defined as the energy released during the cracking of a brittle or ductile material [6]. To determine the evolution of the semi-infinite crack, several researchers used the principle of J-integral [7-8]. Experimental and numerical results show that macroscopic specimens which contain microscopic defects producing local stress concentrations [9-10]. In brittle materials, the failure is considered to be an energy-consuming phenomenon, taking into account the energy state of the atoms before and after cracking. [11]. This study is divided to two parts;

- The first part is devoted to the study of the orientation of the microcrack around the semi-infinite crack according to the angle , whose strain energy is determined for each position of the microcrack.
- On the other hand, the orientation of the microcrack around itself (according to the angle α) is studied in the second part.

According strain energy results, the positioning of the microcrack can amplify, reduce and sometimes stop the propagation of the semi-infinite crack.
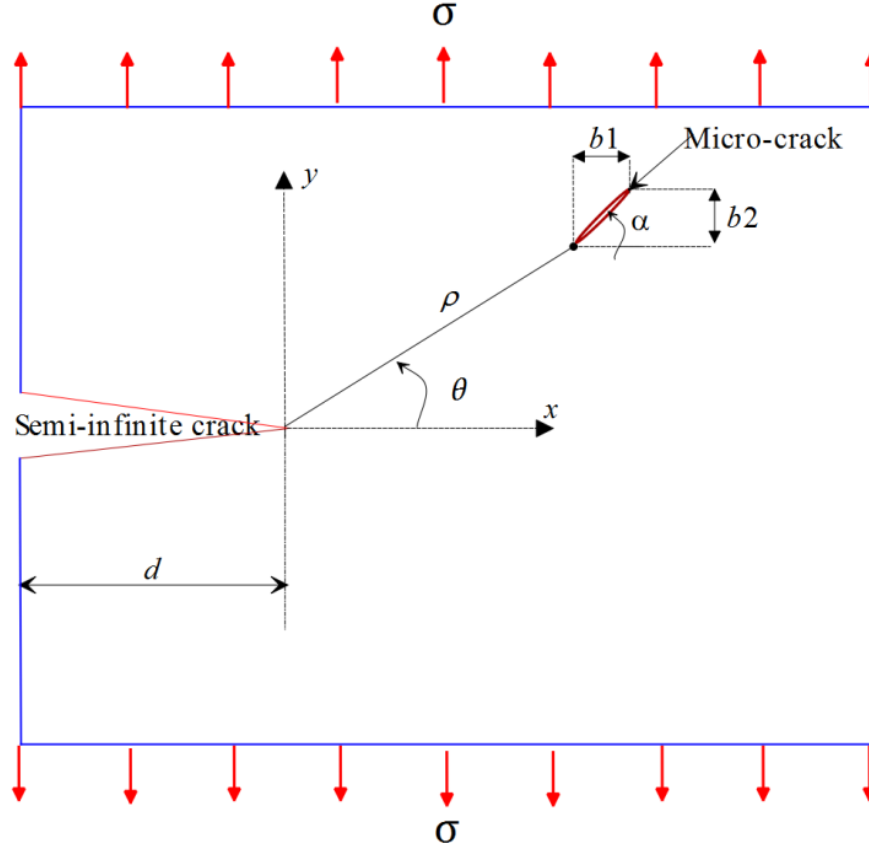
1

Fig. 1 Presence of semi-infinite crack and microcrack in the plane element

where ρ : distance between the semi-infinite crack and micro-rack. d ; semi-infinite crack length. b_1 and b_2 ; dimensions of the micro-crack along the x and y axis successively.

II. Brittle failure

The brittle failure occurs suddenly by cleavage generated during separation of the atoms forming the material [12]. In brittle metals, it is experimentally observed that failure only occurs if the material plasticizes, which shows that microcracks or defects are created during the plasticization of the material [13]. The sudden failure strength of a brittle material is determined by the critical value of the stress intensity factor in mode I (K_I). It varies according to the chemical composition and the property of the cracked material [14]. The stress intensity factor in mode I, can be linearly calculated by the stresses which tend towards infinity at the end of semi-infinite crack [15]. It makes to determine the size of microcrack and effective in stopping of the cracking and consequently controlling the necessary and sufficient qualities [16]. The K_I represents a physical characteristic of the material determined experimentally under conditions [17]. In linear elasticity, the distribution of the plane stresses in the vicinity of the semi-infinite crack is expressed in polar coordinates [18] :

$$\sigma_{ij(r, \ \theta)} = \frac{K_{ij(r)}}{\sqrt{2\pi r}} f_{ij(\theta)} (1)$$

II. 1 Brittle failure theory

For a element of elastic material having a semi-infinite crack, the propagation of this one modifies the surface of their lips. Griffith [11] approached the energy problem and thus proposed a theory of failure based on

2

energy consumption during the crack propagation process. The total energy conservation of the cracked system is given as follows [19]:

$$dW_t = dW_e + dW_{ex} + dW_s + dW_k = 0 \ (2)$$

where, dW_e ; elastic energy, dW_{ex} ; potential energy due to external forces, dW_s ; separation energy, dW_k ; kinetic energy.

In case of kinetic energy greater than zero ($dW_k > 0$), the semi-infinite crack will unstably propagates. The energy rate is defined as being the energy released during the propagation of the semi-infinite crack [20]. By definition, it is given as follows:

$$G = -\frac{\partial}{\partial S}(W_e + W_{ex})(3)$$

According to Griffith [11], the propagation of the semi-infinite crack is ensured when the energy rate is greater than twice the characteristic surface energy of the material (G > 2). Irwin [21] used the term surface energy or energy absorbed in the fracture process to apply it to plastic materials. It also showed that at the crack tip, there is a relation between the strain energy rate and the stress intensity factor.

II. 2 Different modes of fracture

The semi-infinite crack can propagates according to three modes of displacement of the lips of the opening [22]. It can also be propagated according to the mixed mode representing the superposition of two or three modes [23]. Figure 2 illustrates the three modes of displacement of the crack lips. In the first mode of fracture (Mode I), the surfaces of the semi-infinite crack tends to step aside perpendicularly with respect to the plane of crack [24]. Mode II is considered, if the surfaces of the semi-infinite crack slide between it parallel to the plane of crack [25]. On the other hand, mode III occurs when the surfaces of semi-infinite crack slide between it perpendicular to those of mode II [26].

Fig.2 three modes of fracture

For each mode of fracture, the stress intensity factor is determined as a function of the component of constraints. When the point of application of constraints tends towards zero (r - 0), the stress intensity factor is found as follows:

$$\begin{cases} K_I = \sqrt{2\pi r}\sigma_{22} \\ K_{II} = \sqrt{2\pi r}\sigma_{21} \quad (4) \\ K_{III} = \sqrt{2\pi r}\sigma_{23} \end{cases}$$

II. 3 Elastic deformation of material

The deformation of a material is generated during that is subjected to mechanical stresses. it characterizes the behavior of the material [27]. The deformation capacity of an element depends on the nature of the material and shape of the piece while respecting the manufacturing processes [28]. The Figure 3 shows a volume element subjected to triaxial traction along the x, y and y axes.
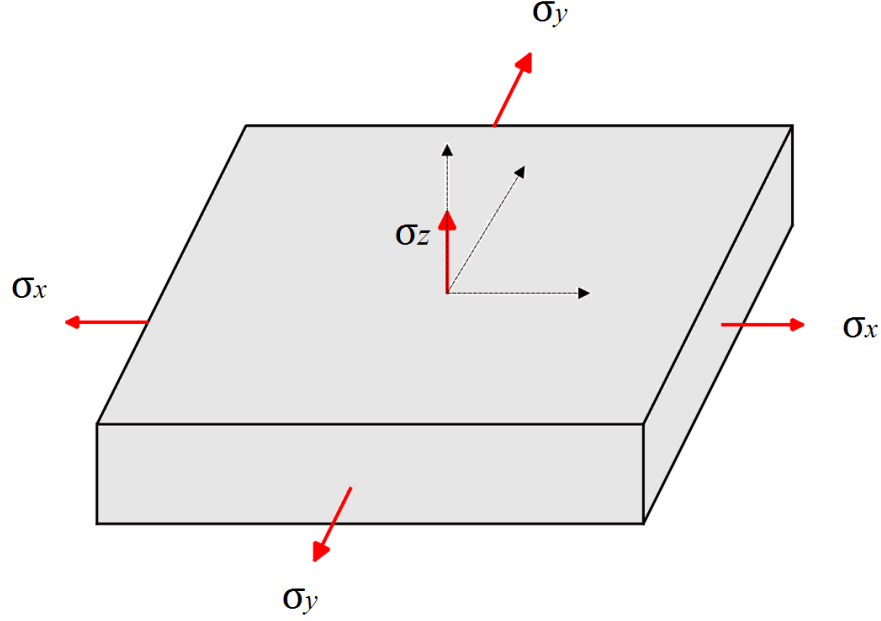
Fig. 3 Traction of an volume element

To determine the deformations corresponding to the stresses applied to this volume element, we use the principle of superposition [29]. The elastic deformation of a material is only given with constraints, the relationship between stress and strain can be written in the following matrix form:

$$[\varepsilon] = \frac{1}{E}
\begin{bmatrix}
1 & -\nu & -\nu & 0 & 0 & 0 \\
-\nu & 1 & -\nu & 0 & 0 & 0 \\
-\nu & -\nu & 1 & 0 & 0 & 0 \\
0 & 0 & 0 & 1+\nu & 0 & 0 \\
0 & 0 & 0 & 0 & 1+\nu & 0 \\
0 & 0 & 0 & 0 & 0 & 1+\nu
\end{bmatrix} * [\sigma] \quad (5)$$

where ε_{ij} ; axial strain, ν ; poisson ratio, E ; elasticity modulus of material.

III. Interaction between microcrack and a semi-infinite crack

The interaction between microcrack and a semi-infinite crack, generates a high concentration of stress, straints and displacements at the crack tip [30]. The semi-infinite crack is determined by their length (l). On the other hand, the microcrack is defined by Burger's vector ($b = b_x + ib_y$). During the propagation of a semi-infinite crack towards the neighboring microcrack, a damage zone surrounding the initial crack occurs with a high concentration of stresses. It is considered to be a highly disturbed area and also called the fracture process zone [31]. The extension of semi-infinite crack is envisaged in a small zone near to the initial crack in which, a strain energy is released [32]. The elastic behavior of cracking during the presence or absence of micro-crack has been studied by several researchers from various disciplines such as metallurgy, mechanics, physics [33-35]. In our case, the interaction is ensured by a semi-infinite craeck with a neighboring microcrack varies around the crack tip with angle and around itself with angle α (see Figure 1). The loading is applied according to the first mode of fracture which opens the crack perpendicular to their lips (Mode I).

4

The mathematical problem of the interaction (crack-dislocation) is formulated in terms of complex potentials of plane stress [36]. The total plane constraints generated by this interaction, are given as a function of global complex potentials;

$$\sigma_{11} + \sigma_{22} = 2\left[\phi'_O(z) + \overline{\phi'_O(z)}\right] (6)$$

$$\sigma_{22} - \sigma_{11} + 2i\sigma_{12} = 2\left[\overline{z}\phi''_O(z) + \psi'_O(z)\right] (7)$$

with

$$\phi_O(z) = \phi_{SIC}(z) + \phi_d(z) (8)$$

$$\psi_O(z) = \psi_{SIC}(z) + \psi_d(z) (9)$$

where $\phi_{SIC}(z), \psi_{SIC}(z)$; complex potential functions of semi-infinite crack. $\phi_d(z), \psi_d(z)$;

complex potential functions of microcrack, $\phi_{Int}(z), \psi_{Int}(z)$; presentents the complex

potential functions of the interaction between semi-infinite crack and microcrack.

III.1 Constraints field

The constraints field generated during the interaction between the semi-infinite crack and neiboring microcrack, represents the superposition of two constraints fields produced by the semi-infinite crack and the microcrack [37]. The constraints found at semi-infinite crack tip, are characterized by a factor called stress intensity factor (SIF). The orientation of microcrack around semi-infinite crack, can generate the stress and consequently release the energies in each zone of the material [38]. Using Equations (6) to (9), H. Hamli Benzahar [4] determined the constraints field of interaction between microcrack and a semi-infinite crack in the following form:

$$\sigma_{11} = \frac{2\mu b}{\pi(1+k)\rho}\left[4sin(\alpha - \theta) - sin(\alpha + \theta) - sin(\theta)\cos(\alpha - 2\theta)\right] (10)$$

$$\sigma_{22} = \frac{2\mu b}{\pi(1+k)\rho}\left[\sin(\alpha + \theta) + sin(\theta)\cos(\alpha - 2\theta)\right] (11)$$

$$\sigma_{12} = \frac{2\mu b}{\pi(1+k)\rho}\left[\cos(\alpha + \theta) - 2sin(\alpha - \theta) + sin(\theta)\sin(\alpha - 2\theta)\right] (12)$$

III. 2 Strain energy release

The semi-infinite crack propagates during the rate of release of the stored elastic strain energy is equal to the rate of creation of strain energy of the crack area [39]. The released strain energy is defined as being the released energy during the propagation of the semi-infinite crack at presence of a neighboring dislocation [40]. Based on the energy state of atoms before and after cracking, Griffith has shown that failure is an consuming phenomenon of energy [11]. Using mathematical approaches, Rice [7] used a scalar quantity called J-integral which predicts that the rate of energy release increases proportionally with the propagation of the semi-infinite crack at presence of the disturbance zone. Consequently, the J-integral can be used to determine the rate of energy release related to the translational deformation of the damage zone at crack tip [41]. This energy is applied to materials with brittle behavior and it is considered to be an essential parameter of failure [6]. In linear elasticity, the strain energy is given by the following formula according to constraints and strains of material [42]:

$$W = \frac{1}{2}\left(\sigma_{11}\varepsilon_{11} + \sigma_{22}\varepsilon_{22} + 2\sigma_{12}\varepsilon_{12}\right) (13)$$

In a brittle material, the external loads produce very high constraints but the strains are very small, that is to say ; $\varepsilon_{11} \simeq \varepsilon_{12} \simeq \varepsilon_{22} \simeq \varepsilon \simeq 0$. For this reason, the strain energy (Equation (13)) can be written in the following form:

$$W = \frac{\varepsilon}{2}\left(\sigma_{11} + \sigma_{22} + 2\sigma_{12}\right) (14)$$

Based on the plane constraints, one can determine the strain energy generated by the interaction between the semi-infinite crack and the neighboring microcrack. The substitution of Equations (10) to (12) into Equation (14), brings us the energy of deformation under the following expression:

$$W = \frac{2.\mu b\varepsilon}{\pi(1+k)\rho} \left[\cos\left(\alpha + \theta\right) + sin\left(\theta\right)\sin\left(\alpha - 2\theta\right)\right] (15)$$

III.2.1 Orientation of the micro-crack around the semi-infinite crack

The orientation of the microcrack around itself and around semi-infinite crack, gives the strain energy in each point of the material. By fixing the orientation of microcrack around itself and varying the orientation angle of microcrack around the semi-infinite crack, the following figures (figure 4(a,b) to 8(a,b)) present the strain energy values found around the semi-infinite crack.
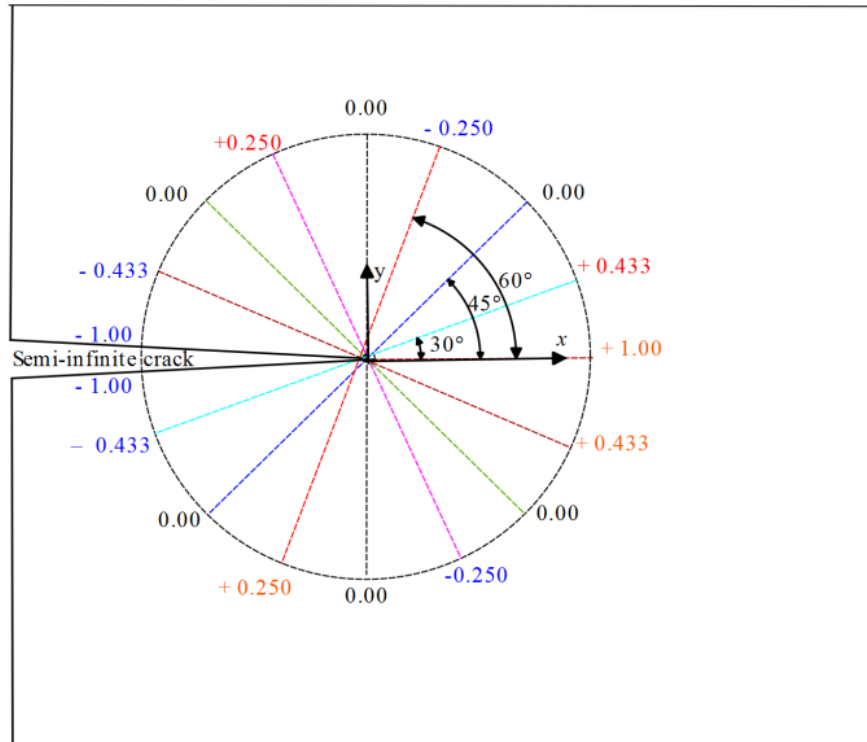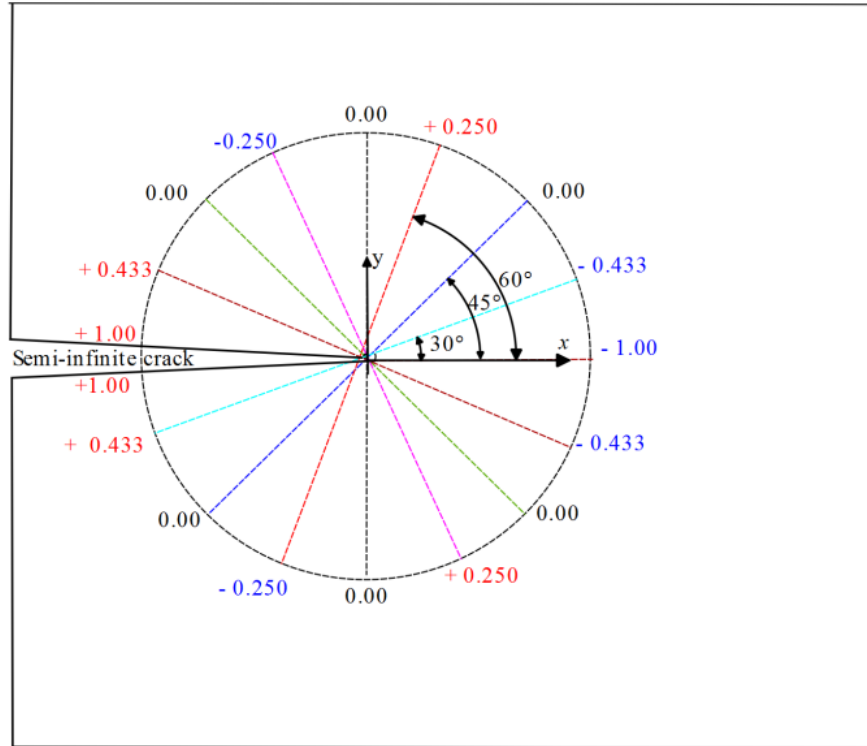
a) b)

Fig.4 Strain energy values around the semi-infinite crack (case of micro-crack is parallel to the semi-infinite crack); a) = 0, b) = π
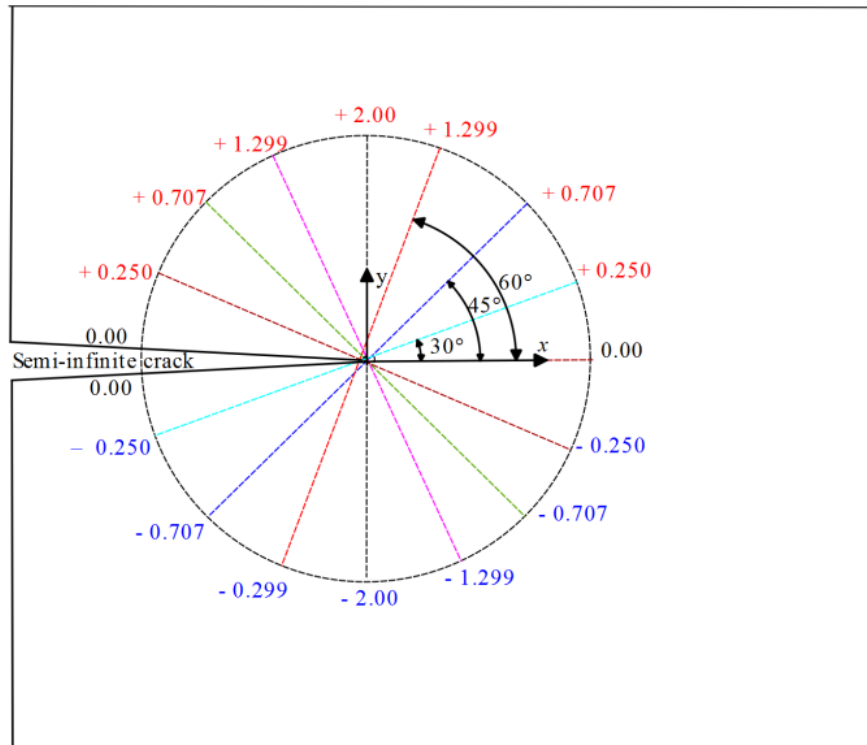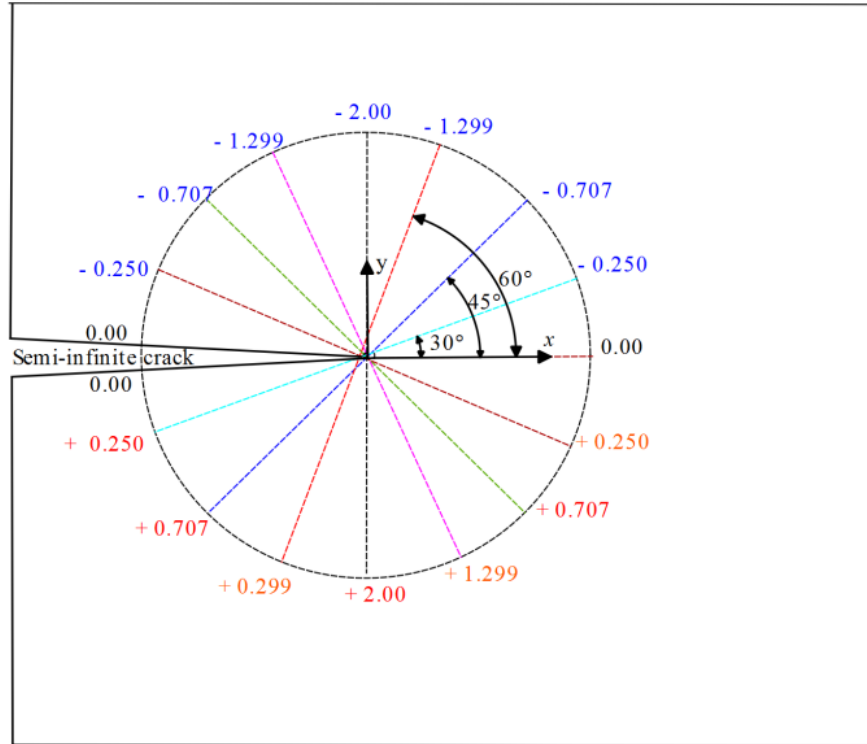
a) b)

Fig. 5 Strain energy values around the semi-infinite crack (case of micro-crack is perpendicular to the semi-infinite crack) ; a) =π/2, b) = 3π/2

a) b)
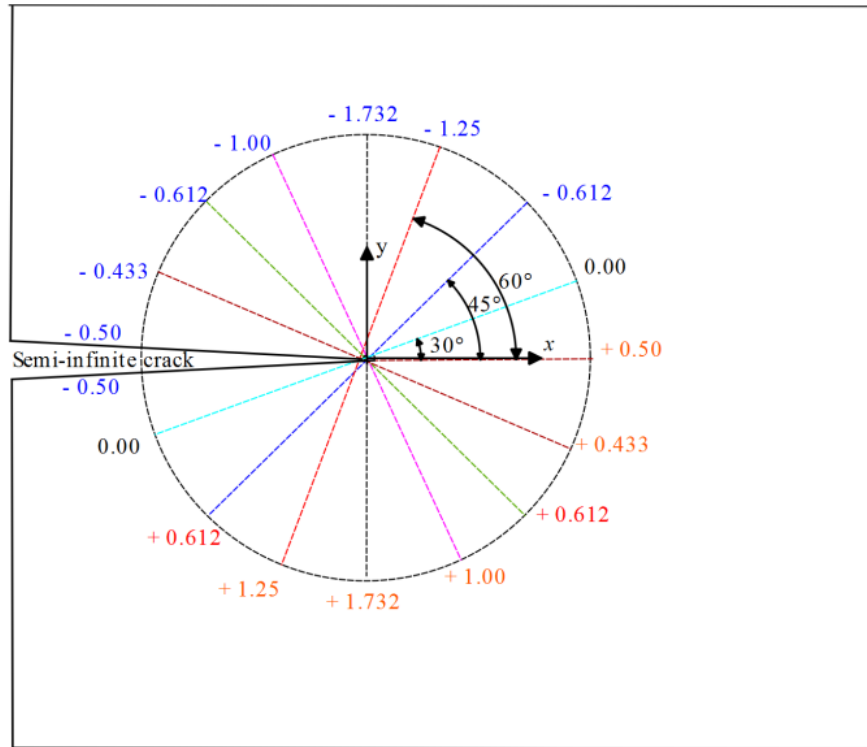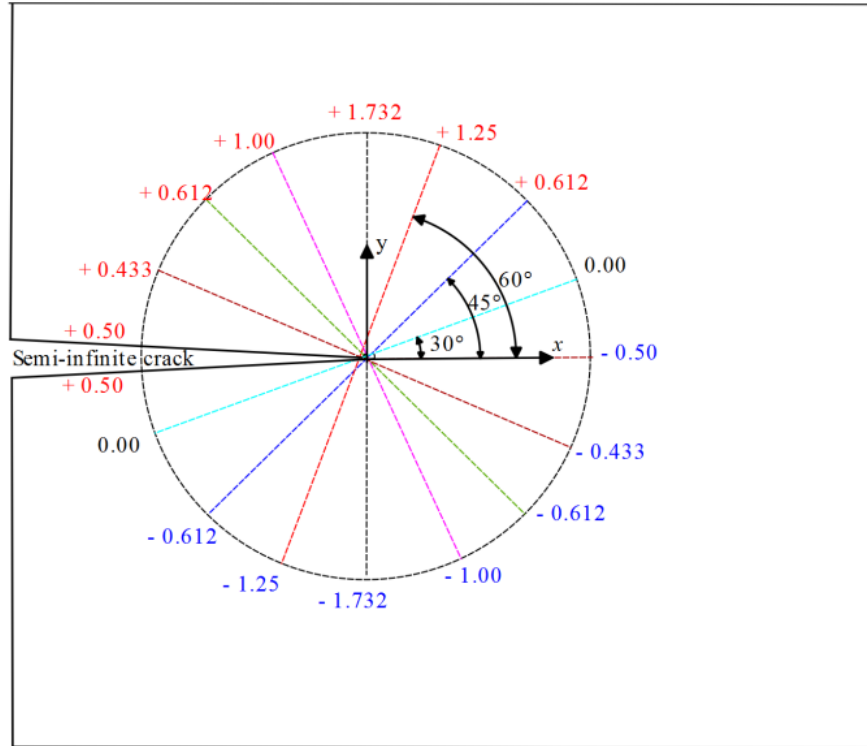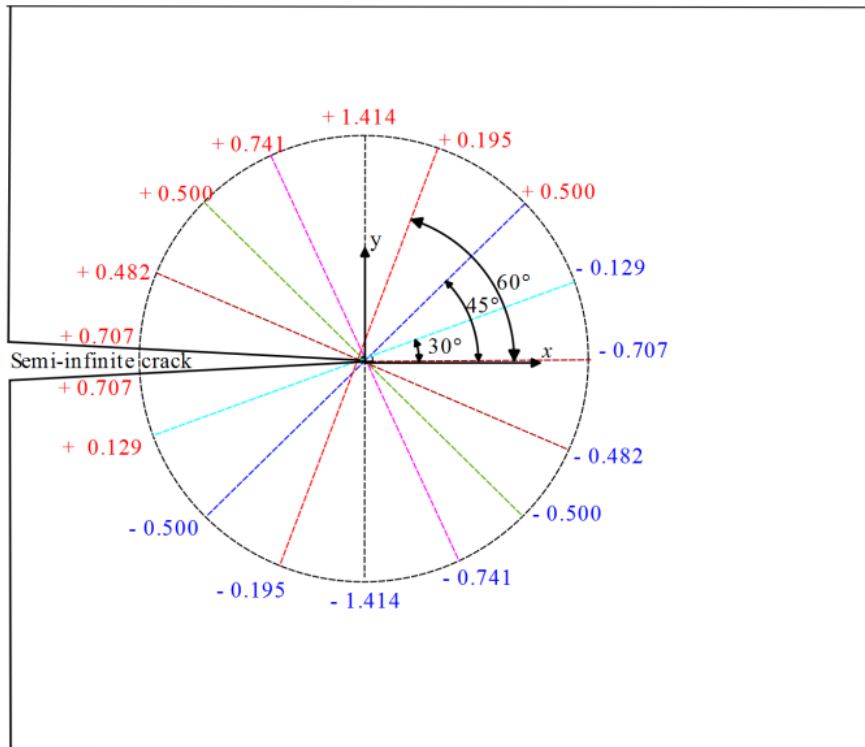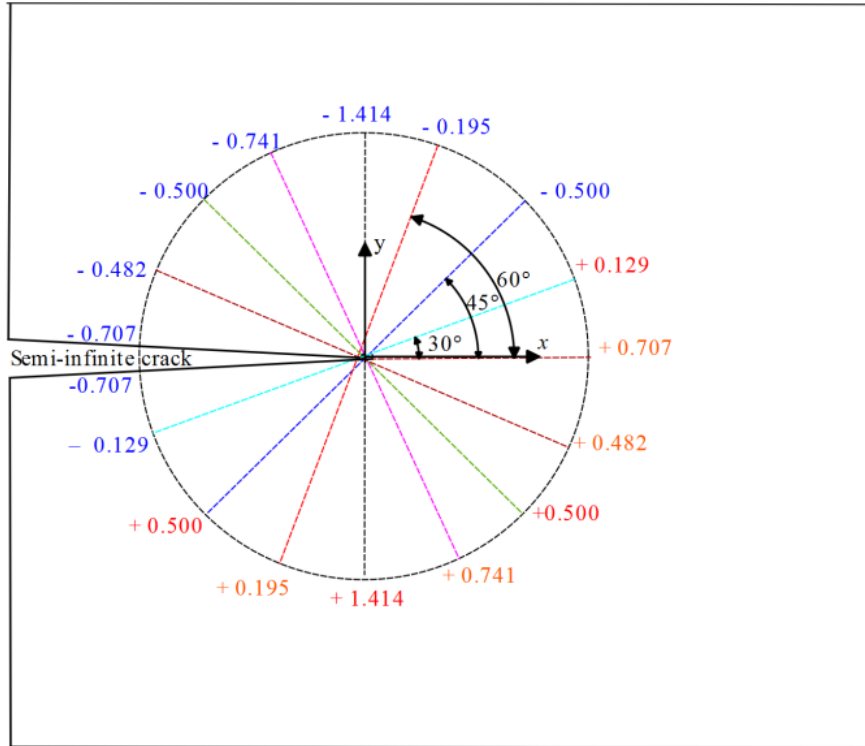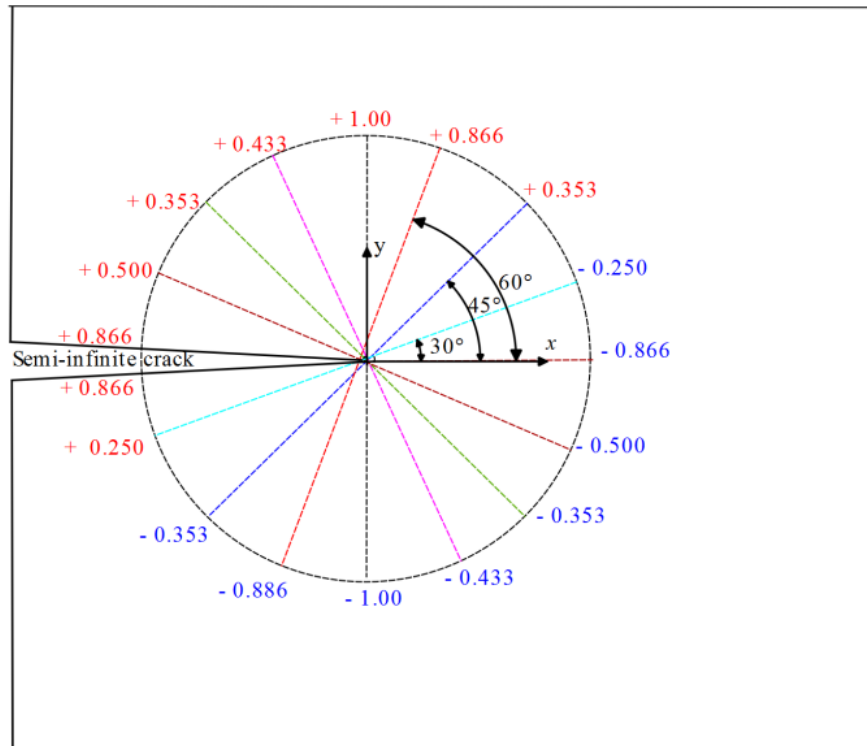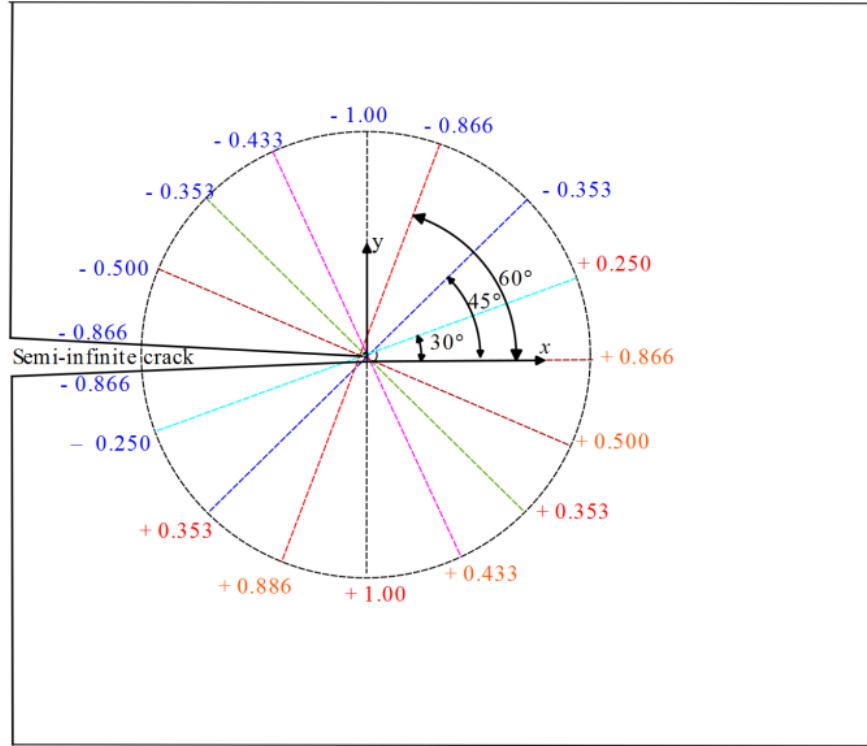
Fig.6 Strain energy values around the semi-infinite crack; a) $=\pi/3$, b) $= -\pi/3$

a) b)

Fig.7 Strain energy values around the semi-infinite crack; a) $=\pi/4$, b) $= -\pi/4$

a) b)

Fig.8 Strain energy values around the semi-infinite crack; a) =π/6, b) = -π/6

by fixing the angle of orientation of the micro-crack around herself, the Figures 9 to 12 show the variation of strain energy according to the angle of orientation of micro-crack around the semi-infinite crack.

Hosted file

`image16.wmf` available at https://authorea.com/users/348620/articles/473833-influence-of-micro-crack-on-the-propagation-of-a-semi-infinite-crack

Fig. 9 Strain energy vs. orientation angle of the micro-crack around the semi-infinite crack ; case of micro-crack is parallel to the semi-infinite crack

Hosted file

`image17.wmf` available at https://authorea.com/users/348620/articles/473833-influence-of-micro-crack-on-the-propagation-of-a-semi-infinite-crack

Fig. 10 Strain energy variation as function of the orientation angle of the micro-crack around the semi-infinite crack ; in case of micro-crack is perpendicular to the semi-infinite crack

Hosted file

`image18.wmf` available at https://authorea.com/users/348620/articles/473833-influence-of-micro-crack-on-the-propagation-of-a-semi-infinite-crack

Fig. 11 Strain energy variation as function of the orientation angle of the micro-crack around the semi-infinite crack ; in case of micro-crack is inclined by $\pi/4$ compared to semi-infinite crack.

Hosted file

`image19.wmf` available at https://authorea.com/users/348620/articles/473833-influence-of-micro-crack-on-the-propagation-of-a-semi-infinite-crack

Fig. 12 Strain energy vs. orientation angle of the micro-crack around the semi-infinite crack ; case of micro-crack is inclined by $\pi/6$ compared to semi-infinite crack.

III.2.2 Orientation of micro-crack around itself

The orientation of microcrack around itself generates constraints, displacements, strain energy and consequently influence on the propagation of the crack [3]. In this case, one maintains the orientation angle of microcrack around semi-infinite crack and varies the orientation of this microcrack around itself, the Figures13 to16 show the variation of the strain energy as a function of the orientation angle of the microcrack around itself.

Hosted file

`image20.wmf` available at https://authorea.com/users/348620/articles/473833-influence-of-micro-crack-on-the-propagation-of-a-semi-infinite-crack

Fig. 13 Strain energy vs. orientation angle of the micro-crack around itself

; case of micro-crack is parallel and perpendicular compared to$x$-x axis.

Hosted file

`image21.wmf` available at https://authorea.com/users/348620/articles/473833-influence-of-micro-crack-on-the-propagation-of-a-semi-infinite-crack

Fig. 14 Strain energy vs. orientation angle of the micro-crack around itself

; case of micro-crack is inclined by $\pi/3$ compared to x-x axis.

Hosted file

`image22.wmf` available at https://authorea.com/users/348620/articles/473833-influence-of-micro-crack-on-the-propagation-of-a-semi-infinite-crack

Fig. 15 Strain energy vs. orientation angle of the micro-crack around itself

; case of micro-crack is inclined by $\pi/4$ compared to x-x axis.

Hosted file

`image23.wmf` available at https://authorea.com/users/348620/articles/473833-influence-of-micro-crack-on-the-propagation-of-a-semi-infinite-crack

Fig. 16 Strain energy vs. orientation angle of the micro-crack around itself

; in case of micro-crack is inclined by $\pi/6$ compared to x-x axis.

Results and discussions

In this research, the results of strain energy found during the positioning of micro-crack with respect to the semi-infinite crack, limit areas of amplification, reduction and sometimes arrest of the propagation of semi-infinite crack.

- According to Figures 4 (a, b) - 8 (a, b), whatever the positioning of micro-crack compared to the semi-infinite crack ($\forall \alpha \, \epsilon \, [0 \, , \, 2\pi]$ and $\forall \theta \, \epsilon \, [0 \, , \, 2\pi]$), the values of strain energy are symmetrical with respect to the point of semi - infinite crack.
- From Figure 4 (a, b), in case of the micro-crack is parallel with respect to the semi-infinite crack ($= 0$ et $= \pi$), the strain energy is zero if this micro-crack is located on the axis y-y ($= 90°$ and $= 270°$), and reaches the maximum value when this micro-crack is located in axis x-x ($= 0°$ et $= 180°$).
- On other, the Figure 5 (a, b) represents a micro-crack perpendicular to the semi-infinite crack ($= \pi/2$ et $= 3\pi/2$). The strain energy is zero if the micro-crack is located on the x-x axis and reaches the maximum value when this micro-crack is located on the y-y axis.
- Figures 9-12 represent variation of the strain energy and consequently the amplification or reduction of the propagation of semi-infinite crack according to the orientation of micro-crack around itself and around semi-infinite crack. The Table 1 summarizes the areas of amplification, reduction and also arrest of propagation of the semi-infinite crack.

Table 1 area of amplification, reduction and arrest of the propagation of the semi-infinite crack

Figures	(°)	α (rad)	Effect	α (rad)	Effect
Figure 9	[0 − 45]	0	Amplified	π	Reduce
	[45- 90]		Reduce		Amplified
	[90 − 135]		Amplified		Reduce
	[135 -225]		Reduce		Amplified
	[225-270]		Amplified		Reduce
	[270-315]		Reduce		Amplified
	[315-360]		Amplified		Reduce
Figure 10	[0 - 11]	$\pi/2$	Arrest	$3\pi/2$	Arrest
	[11 - 166]		Reduce		Amplified
	[166 - 192]		Arrest		Arrest
	[192 - 349]		Amplified		Reduce
	[349 −360]		Arrest		Arrest
Figure 11	[0 − 34]	$\pi/4$	Amplified	$5\pi/4$	Reduce
	[534 −215]		Reduce		Amplified

14

Figures	(°)	α (rad)	Effect	α (rad)	Effect
	[215 –360]		Amplified		Reduce
	[0 – 149]	3π/4	Reduce	7π/4	Amplified
	[149- 327]		Amplified		Reduce
	[327 –360]		Reduce		Amplified
Figure 12	[0 - 37]	π/6	Amplified	7π/6	Reduce
	[37- 215]		Reduce		Amplified
	[215 –360]		Amplified		Reduce
	[0 – 29]	π/3	Amplified	4π/3	Reduce
	[29 – 212]		Reduce		Amplified
	[212 –360]		Amplified		Reduce
	[0- 150]	2π/3	Reduce	5π/3	Amplified
	[150- 329]		Amplified		Reduce
	[329 –360]		Reduce		Amplified
	[0- 143]	5π/6	Reduce	11π/6	Amplified
	[143- 324]		Amplified		Reduce
	[324 –360]		Reduce		Amplified

By maintaining the positioning of micro-crack with respect to semi-infinite crack and varying the orientation of this micro-crack around itself, Figures 13-16 represents the effect of the micro-crack on the strain energy and the propagation of semi-infinite crack. Table 2, groups the zones of amplification and reduction of semi-infinite crack

Table 2 Amplification and reduction zones of propagation of semi-infinite crack according to the orientation of micro-crack around itself

Figures	α (°)	(rad)	Effect	(rad)	Effect
Figure 13	0- 90	0	Amplified	π	Reduce
	90- 270		Reduce		Amplified
	270 – 360		Amplified		Reduce
	0- 180	π/2	Amplified	3π/2	Reduce
	180- 360		Reduce		Amplified
Figure 14	0- 166	π/3	Reduce	4π/3	Amplified
	166- 349		Amplified		Reduce
	349 – 360		Reduce		Amplified
	0- 11	2π/3	Amplified	5π/3	Reduce
	11- 192		Reduce		Amplified
	192 – 360		Amplified		Reduce
Figure 15	0- 180	π/4 and 5π/4	Reduce	3π/4 and 7π/4	Amplified
	180- 360		Amplified		Reduce
Figure 16	0-60	π/6	Reduce	7π/6	Amplified
	60- 240		Amplified		Reduce
	240-360		Reduce		Amplified
	0-122	5π/6	Reduce	11π/6	Amplified
	122-300		Amplified		Reduce
	300-360		Reduce		Amplified

According to Table 1, the presence of microcrack in vicinity of the semi-infinite crack, can amplify, reduce and also arrest the propagation of semi-infinite crack. whatever the positioning of microcrack with respect to the

semi-infinite crack ($\forall \alpha \; \epsilon \; [0 \; , \; 2\pi]$ and $\forall \theta \; \epsilon \; [0 \; , \; 2\pi]$), the tables 3-4 summarize the amplification, reduction zones and arresting the propagation of the semi-infinite crack.

Table 3 Amplification and reduction zones of the propagation of semi-infinite crack.

In case ; $\alpha \; \epsilon [0, \; \pi/2[\cup \;]\pi/2, \; \pi] \cup [\pi, \; 3\pi/2[\cup]3\pi/2, \; 2\pi]$ and $\forall \theta \; \epsilon \; [0 \; , \; 2\pi]$

α (rad)	($\degree$)	Effect
$[0, \pi/2[$	$0-30$	Amplified
	45- 90	Reduce
	$315-360$	Amplified
$]\pi/2, \pi]$	0- 45	Reduce
	150- 215	Amplified
	330– 360	Reduce
$[\pi, 3\pi/2[$	0- 30	Reduce
	45- 90	Amplified
	315– 360	Reduce
$]3\pi/2, 2\pi]$	0- 45	Amplified
	150- 215	Reduce
	330– 360	Amplified

Table 4 Amplification, reduction and arrest zones of the propagation of semi-infinite crack.

In case of ; $\alpha = \pi/2$, $\alpha = 3\pi/2$ and $\forall \theta \; \epsilon \; [0 \; , \; 2\pi]$

($\degree$)	Efect	Efect
	$\alpha = \pi/2$	$\alpha = 3\pi/2$
[0 - 11]	Arrest	Arrest
[11 - 166]	Reduce	Amplified
[166 - 192]	Arrest	Arrest
[192 - 349]	Amplified	Reduce
[349 – 360]	Arrest	Arrest

Conclusion

In this research work, the main objective is to determine the effect of micro-crack on the semi-infinite crack by determining the strain energy and limiting the zones of amplification, reduction and sometimes arrest of propagation of semi-infinite crack. According to the Figures 4-16, whatever the positioning of the micro-crack compared to semi-infinite crack, the strain energy values are symmetrical with respect to the semi-infinite crack tip. The results of strain energy summarized in Tables 1- 4, show that the zones of amplification, reduction and arrest of propagation of semi-infinite crack are symmetrical compared to the point of semi-infinite crack tip. By varying the orientation angles (and α), the Table 3 summarizes all zones of amplification and reduction and presents a symmetry in the effect on the propagation of semi-infinite crack ($\alpha \quad [0 \; , \; \pi/2]$ symmetrical with$\alpha \quad [\pi \; , \; 3\pi/2]$ and$\alpha \quad]\pi/2, \pi]$ σψμμετριςαλ ωιτη α $]3\pi/2, 2\pi]$). Αςςορδινγ το Ταβλε 4, τηε πρεσενςε οφ μιςρο-ςραςκ ιν α περπενδιςυλαρ ποσιτιον το τηε σεμι-ινφινιτε ςραςκ (τηατ ις το σαψ · $\alpha = \pi/2$ and $\alpha = 3\pi/2$), can also arrest the propagation of crack in the zones ; ϑ $[0 \; , \; 11]$, $[166\degree - 192\degree]$ and $[349\degree - 360\degree]$.

References

1. A. A. Rubinstein. Macrocrack-Microdefect Interaction. *J. Appl. Mech.* 1986 ; 53 :505-510.

16

2. Sham-Tsong Shiue and Sanboh Lee. The elastic interaction between screw dislocations and cracks emanating from an elliptic hole. *J. of Appl. Phys* . 1988 ; 64 :129.

3. Xiaotao Li, Hongda Yang, Xiaodong Zan, Xu Li and Xiaoyu Jiang. Effect of a micro-crack on the kinked macro-crack. *Theor. Appl. Fract. Mech.* 2018 ; 96 : 468-475.

4 Hamid Hamli Benzahar. Theoretical and numerical analysis of stress and stress intensity factor in bi material. Int. J. Struct. Integr. 2019 ; 10 : 76-84.

5. T. Y. Zhang and J. C. M. Li. Interaction of an edge dislocation with an interfacial Crack. *Int. J. Appl. Phys.* 1992; 72 ;2215.

6. Ankang Cheng, Nian-Zhong Chen and Yongchang Pu. An energy principles based model for fatigue crack growth prediction.*Int.. J. of Fat*, 2019;128 : 105198.

7. J. R. Rice. A Path Independent Integral and the Approximate Analysis of Strain Concentration by Notches and Cracks.*J. Appl. Mech* . 1968; 35: 379-386.

8. Dorothee Knees. Griffith-formula and j-integral for a crack in a power-law hardening material.*Math. Models Meth. Appl. Sciences.* 2006; 16 : 1723-1749.

9. D.V. Bambill, C.A. Rossit and A. Susca. Numerical experiments on the determination of stress concentration factors in orthotropic perforated plates subjected to in - plane loading. *Struct. Eng. Mech* . 2009 ; 32 ; 549-561.

10. H. Hamli Benzahar and Mohamed Chabaat. Damage Zone Size Limit During the Crack Propagation. *Period. Polyt. Civil Eng.* 2020; 64 : 73–80.

11. A. A.Griffith. The phenomana of rupture and flow in solid, Philosophical translation. *Royal Soc of London, Serie A* . 1921; 221: 163-198.

12. Škec, L., Alfano, G. & Jelenić, G. Complete analytical solutions for double cantilever beam specimens with bi-linear quasi-brittle and brittle interfaces. *Int. J. Fract* . 2019 ; 215 : 1–37.

13. Tian-hu Hao. Cod of a crack in viscoelastic perfectly plastic material. *Int. J. Fract..* 1992 ; 56.

14. Rong Luo and Hui Chen. An improved method of characterizing fracture resistance of asphalt mixtures using modified Paris' law: Part II—Establishment of index for fracture resistance. *Mech. Mater.* 2019 ; 138 ;103168.

15. Mohammad Hossein Ahmadi and Hamed Molladavoodi. A micromechanical Sliding-Damage Model Under Dynamic Compressive Loading. *Period Polyt. Civil Eng* . 2019 ; 63 : 168–183.

16. W.-S. Lei. Statistics of single-fibre tensile strength incorporating spatial distribution of microcracks. *Fract Eng Mater Struct* . 2016 ; 39 :1337-1351.

17. Reaz A. Chaudhuri. On through-thickness distribution of stress intensity factors and energy release rates in the vicinity of crack fronts.*Engineering Fracture Mechanics.* 2019 ; 216 : 106478.

18. Williams, M. L. On the Stress Distribution at the Base of a Stationary Crack. *J. Appl. Mech* . 1956 ; 24 : 109-114.

19. Atkinson, C. and Eshelby J. D. The flow of energy into the tip of a moving crack. *Int. J. Fract* . 1984 ; 26 : 316–321.

20. X. G. Wang, H. R. Ran, C. Jiang and Q. H. Fang. An energy dissipation-based fatigue crack growth model,*Int. J. Fat.* 2018 ; 114 : 167-176.

21. G. Irwin. Analyses of stresses and strains near end of crack traversing a plate. *J. Appl. Mech* . 1957 ; 24 :351-369.

22. Hadei, M. R., Kemeny, J., Ghazvinian, A., Rezaiepoor, A., Sarfarazi, V. New Development to Measure Mode I. Fracture Toughness in Rock.*Period. Polyt. Civil Eng* . 2017 ; 61 : 51-55.

23. Seyed Mohammad Javad Razavi and Filippo Berto. A new fixture for fracture tests under mixed mode I/II/III loading. *Fat. Fract. Eng. Mater. Struct* . 2019 ; 42 : 1874-1888.

24. Iarley Loan SampaioLibos and Liang Cui. Effects of curing time, cement content, and saturation state on mode-I fracture toughness of cemented paste backfill.*Eng. Fract. Mech.* 2020 ; 235 : 107174.

25 Victor I. Rizov. Non-linear study of mode II delamination fracture in functionally graded beams. *Steel Comp. Struct.* 2017 ; 23 : 263-271.

26. Mojtaba Mahmoudi Monfared. Mode III SIFs for interface cracks in an FGM coating-substrate system. *Struct. Eng. Mech* . 2017 ; 64 : 71-79.

27. Alexey Nikolaevich Savkin, Alexander Alexandrovich Sedov and Artem Valerievich Andronik. The steel damageability simulation under random loading by the power, energetical and strain fracture criterions,*Period. Polyt. Mech. Eng.* 2014; 58: 119-126.

28. Liu Zhenyu, Wang Chuang, Duan Guifang and Tan Jianrong. A new refined plate theory with isogeometric approach for the static and buckling analysis of functionally graded plates.*Int. J. Mech. Sciences.* 2019 ; 162 : 105036.

29. S.S Bhadauria, M.S Hora, K.K Pathak. Effect of Stress Triaxiality on Yielding of Anisotropic Materials under Plane Stress Condition. *J. Solid Mech* . 2019 ; 1 : 226-232.

30. H. Hamli Benzahar and M. Chabaat. Crack in brittle material at presence of a dislocation, *Advanc. Mater. Resear* . 2014; 921:2043- 2047.

31. H Hadjab-Souag, J. F. Thimus and Mchabaat. Detecting the fracture process zone in concrete using scanning electron microscopy and numerical modelling using the nonlocal isotropic damage model.*Canad. J. Civil Eng* . 2007; 34: 496-504.

32. P Gallo, T Sumigawa, T Kitamura, F Berto. Evaluation of the strain energy density control volume for a nanoscale singular stress field. *Fat. Fract Eng. Mater Struct.*2016 ; 39 : 1557-1564.

33. Tong-Yi Zhang, J. E. Hack and L. J. Guido. An array of dislocations in a strained epitaxial layer. 1. Elastic energy.*J. appl. phys.* 1994; 75 : 2358-2362.

34. H. Hamli benzahar and M. Chabaat. Stress field and energy analysis during the fracture of composite materials. *Appl. Mech. Mater.*2014; 532 : 524-533.

35. Flavio V.Souza and David H.Allen. Modeling the transition of microcracks into macrocracks in heterogeneous viscoelastic media using a two-way coupled multiscale model. *Int. J. Solids Struct.* 2011; 48: 3160-3175.

36. A. Corfdir and G. Bonnet. Exact degenerate scales in plane elasticity using complex variable methods.*Int. J. Solids Struct.* 2016 ; 80 : 430-444.

37. Ming-Yuan He and John W. Hutchinson. Kinking of a crack out of an interface, Int. J. Appl. Mech. 1989 ; 56 : 270-278.

38. W.-Y. TIAN and Y.-H. CHEN. Arbitrarily oriented microcracks near the tip of an interface macrocrack in bonded dissimilar anisotropic materials. *Fat. Fract. Eng. Mater. Struct* . 2004 ; 27: 379-390.

39. S. SHAHROOI , I. H. METSELAAR and Z. HUDA. Evaluating a strain energy fatigue method using cyclic plasticity models. *Fat. Fract. Eng. Mater. Struct.* 2010 ; 33 : 530-537 .

40. H. Ayas, H. Hamli Benzahar, M. Chabaat, Energy Release Rate during the Cracking of Composite Materials. *Energy Proced* . 2015 ; 74 : 1040-1047.

41. Szekrényes A. J-integral for delaminated beam and plate models. *Period. Polytech. Mech. Eng* . 2012 ; 56 : 63-71.

42. C. O. Horgan. On the strain-energy density in linear elasticity. *J. Eng. Math* . 1973 ; 7 : 231–234.

Hosted file

`tables.rar` available at https://authorea.com/users/348620/articles/473833-influence-of-micro-crack-on-the-propagation-of-a-semi-infinite-crack

Hosted file

`figures.rar` available at https://authorea.com/users/348620/articles/473833-influence-of-micro-crack-on-the-propagation-of-a-semi-infinite-crack